


RESEARCH ARTICLE

Open Access



Seasonal and regional variations of atmospheric ammonia across the South Korean Peninsula

Taehyun Park¹, Rahul Singh¹, Jihee Ban¹, Kyunghoon Kim¹, Gyutae Park^{1,2}, Seokwon Kang¹, Siyoung Choi³, Jeongin Song¹, Dong-Gil Yu¹, Min-Suk Bae⁴, Junyoung Ahn³, Hae-Jin Jung³, Yong-Jae Lim³, Hyun Woong Kim³, Tae Kyung Hwang³, Yu Jin Choi³, Soo-Young Kim³, Hyo Seon Kim³, Yu Woon Chang³, Hye Jung Shin³, Yunsung Lim⁵, Jongtae Lee⁵, Jinsoo Park³, Jinsoo Choi^{3*} and Taehyoung Lee^{1*} 

Abstract

This study aimed to identify the factors causing NH₃ emissions in the South Korean Peninsula and West Sea region. To analyze the trends of NH₃ and other air pollutants, such as NO_x, CO, and NR-PM₁, we collected samples from six supersites across the peninsula, a roadside in Seoul, and the West Sea over different sampling periods, ranging from 1 month to 1 year. The highest NH₃ concentrations were found at rural areas, ascribed to agricultural activities, particularly NH₄NO₃ decomposition at high summer temperatures. Areas with low population densities recorded the lowest NH₃ concentrations, attributed to the lack of anthropogenic activities. A roadside field experiment confirmed the close link between ambient NH₃ and vehicle emissions in urban regions by showing a strong correlation between CO and NO_x concentrations and that of NH₃. Moreover, we examined oceanic emissions near the eastern coast of South Korea in the West Sea. Long-range transportation studies confirmed that most of the pollutants (NH₃, CO, and PM₁) were transported by wind from the northeastern region of China. A maritime origin study showed that oceanic emissions and NH₄NO₃ decomposition in the atmosphere owing to high temperatures were the causing NH₃ pollution. These findings provided valuable insights into the emission sources of NH₃ in primary air pollutants in South Korea, highlighting the contributions of land-based and oceanic sources. Our study can help inform policy-makers and stakeholders for developing effective regional air pollution control strategies.

Keywords NH₃, Seasonal variation, Emission sources, Ammonia concentration, Passive sampler method, Korean Peninsula

*Correspondence:

Jinsoo Choi
reconjs@korea.kr
Taehyoung Lee
thlee@hufs.ac.kr

¹ Department of Environmental Science, Hankuk University of Foreign Studies, Yongin 17035, Korea

² Present Address: Air Pollution Engineering Division, Climate and Air Quality Research Department, National Institute of Environmental Research, Incheon 22689, Korea

³ Air Quality Research Division, Climate and Air Quality Research Department, National Institute of Environmental Research, Incheon 22689, Korea

⁴ Department of Environmental Engineering, Mokpo National University, Muan 58554, Korea

⁵ Transportation Pollution Research Center, National Institute of Environmental Research, Incheon 22689, Korea



© The Author(s) 2023. **Open Access** This article is licensed under a Creative Commons Attribution 4.0 International License, which permits use, sharing, adaptation, distribution and reproduction in any medium or format, as long as you give appropriate credit to the original author(s) and the source, provide a link to the Creative Commons licence, and indicate if changes were made. The images or other third party material in this article are included in the article's Creative Commons licence, unless indicated otherwise in a credit line to the material. If material is not included in the article's Creative Commons licence and your intended use is not permitted by statutory regulation or exceeds the permitted use, you will need to obtain permission directly from the copyright holder. To view a copy of this licence, visit <http://creativecommons.org/licenses/by/4.0/>.

1 Introduction

In the last few decades, there has been significant progress in technology within the agricultural, industrial, and automobile sectors of South Korea and East Asian countries. These advancements have played a crucial role in driving economic growth and improving the quality of life. However, this progress has come at the cost of a deteriorating environmental condition owing to emission of air pollutants, such as ammonia (NH_3), particulate matter (PM), and carbon monoxide (CO) from various sectors (Mukhopadhyay & Forssell, 2005; Singh et al., 2021; Stern, 2015). Atmospheric NH_3 , a major pollutant generated by agricultural activities, contributes significantly to the formation of aerosols in the atmosphere (Huang et al., 2011; Sigurdarson et al., 2018). These aerosols, formed through reactions between NH_3 and organic acids, are mainly responsible for primary air pollution. Moreover, NH_3 has a detrimental effect on the health of marine animals, which ultimately affects human lives (Miller et al., 1990). Furthermore, NH_3 plays a critical role in the formation of secondary PM_{10} (aerodynamic diameter $\leq 10 \mu\text{m}$), as it combines with acidic substances such as nitric acid (HNO_3) and sulfuric acid (H_2SO_4) to form ammonium salts, contributing to the formation of PM in the atmosphere (Huang et al., 2011). The PM_{10} mixture comprises several harmful chemical compounds, including sulfates, nitrates, and organic compounds (Perrone et al., 2014). These inhalable particles pose significant health risks and could cause lung-related diseases such as breathing difficulties and pneumonia (Zhang et al., 2020). CO is produced primarily from incomplete fuel combustion by vehicles and industries (Badr & Probert, 1994; Zhao et al., 2018), and is a major pollutant in urban areas. Although CO is the primary pollutant in vehicle exhaust gases, other pollutants emitted from vehicles have been studied in an effort to improve understanding of the nature of vehicle emissions (Tsai et al., 2006). Although research has focused on industrial and agricultural NH_3 emissions, vehicle emissions contribute significantly to the total emissions of NH_3 in urban areas (Cao et al., 2021). Recent studies have suggested that vehicle emissions, along with NO_x ($\text{NO} + \text{NO}_2$) pollutants, could lead to diverse environmental changes in urban areas (Wang et al., 2020). Such changes cause the rapid growth of new atmospheric pollutants through HNO_3 and NH_3 condensation, enabling the newly formed particulates to persist in highly polluted environments (Wang et al., 2020).

Numerous studies have investigated atmospheric NH_3 concentrations in various regions worldwide, including South Korea. For instance, Kumar et al. (2019) assessed the atmospheric NH_3 concentration in Mumbai, the most populated city in India, and estimated the economic effects of the associated human health issues. Liu et al.

(2014) researched the contribution of vehicle emissions to NH_3 pollution in a traffic-intensive area in an urban tunnel in Guangzhou, China. Chang et al. (2016) verified that vehicle emissions were an important source of NH_3 pollution in the Shanghai region of China. Wang et al. (2015) comprehensively studied the effects of atmospheric NH_3 on air quality in Shanghai, China. Singh et al. (2021) conducted year-round measurements of atmospheric NH_3 in the Seoul metropolitan area, including the urban, suburban, industrial, and agricultural areas. Park et al. (2021) analyzed the role of NH_3 in the formation of PM in South Korea.

Measuring atmospheric NH_3 concentrations by employing the passive sampler method for long-term data collection is a well-established practice (Clark et al., 2020; Park et al., 2021; Puchalski et al., 2011; Singh et al., 2021). Accordingly, to gain a comprehensive understanding of NH_3 trends and the regional characteristics in different seasons, we used a passive sampler to measure NH_3 concentrations through all four seasons in South Korea. In addition, we measured and analyzed the concentrations of other air pollutants, such as NO_x , CO, and PM_{10} in the Seoul and West Sea region, which contributed to our understanding of NH_3 . We consider this study a valuable source for gaining a deeper understanding of the effects of NH_3 over the Korean Peninsula.

2 Methods

2.1 Measurement site

2.1.1 National Institute of Environmental Research supersites

We investigated the regional and seasonal variations in NH_3 concentrations across the Korean Peninsula by conducting measurements at six supersites operated by the National Institute of Environmental Research (NIER) of Korea, covering both urban and remote areas (Fig. 1). Table 1 shows a summary of the site characteristics, including site type, and longitude and latitude. The measurements of NH_3 concentrations were conducted by weekly sampling at the sites for 1 year (June 1, 2020 to July 2, 2021). The Seoul metropolitan area was selected because of its high population density and numerous air pollution sources, including industrial facilities, transportation, and residential activities (Seoul Research Data Service, 2023). The second site is in Daejeon, a major city in the central part of South Korea that serves as a hub for transportation, technology, and industry. This site was chosen to provide information about multiple sources of air pollution in the central region of the country. The Gwangju site was selected to record pollution data from the nearby agricultural and residential areas. The fourth site, Ulsan, the largest industrial city in the country, was chosen primarily for capturing NH_3 emissions from

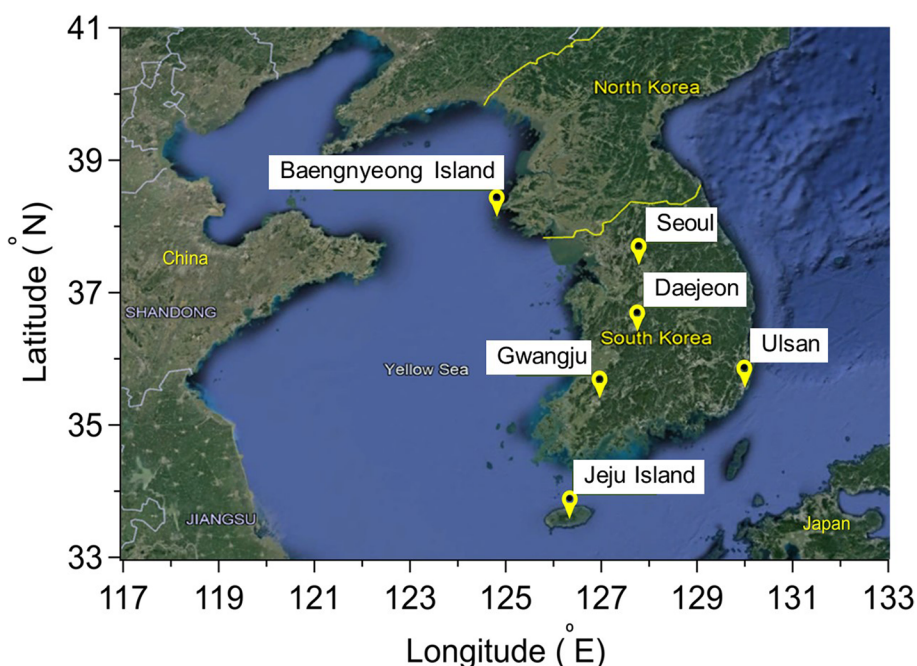


Fig. 1 Satellite image of the National Institute of Environmental Research (NIER) station sites chosen for NH₃ data collection across the Korean Peninsula

Table 1 Detailed information on the location, time periods, and methods used for NH₃ measurements in each site. The top six sites are National Institute of Environmental Research (NIER) supersites

Site name	Period	Type	Latitude	Longitude	Sampling type
Seoul metropolitan area	June 1, 2020 to July 2, 2021	Urban	37.61°	126.93°	Passive
Central region (Daejeon)		Urban	36.32°	127.41°	Passive
Honam area (Gwangju)		Urban	35.23°	126.85°	Passive/URG ^a
Yeongnam area (Ulsan)		Urban	35.58°	129.32°	Passive
Jeju Island		Rural	33.35°	126.39°	Passive
Baengnyeong Island		Rural	37.97°	124.63°	Passive
Hongjimun Tunnel	Aug. and Oct., 2018	Roadside	37.61°	126.97°	Real-time ^b
West Sea	June 2 and 5, 2019	Airborne	37.16°	124.20°	Real-time ^b

^a URG University Research Glassware Denuder

^b Real-time Off-Axis Integrated Cavity Output Spectroscopy (OA-ICOS)

industrial sources. The fifth site, Jeju Island in the West Sea, is characterized by a low population and minimal industrial activity, and was chosen primarily to record pollution transported from the surrounding areas by the wind. The sixth site is on the remote Baengnyeong Island, which has minimal human activity and industrial operations and is located approximately 200 km from the Shandong Peninsula of eastern China (Kang et al., 2020; Lee et al., 2015). As this island is close to China, we expected the local NH₃ measurements to provide exclusive data on the pollution transported from neighboring countries.

2.1.2 Roadside measurement site

Vehicular emissions, such as NH₃, CO, and NO_x, in Seoul were measured at the Hongjimun Tunnel (37.61°N, 126.97°E) on the Naebu Expressway in the Seoul metropolitan area (Figs. 2 and S1). As it is located in a densely populated area, this site experiences a high volume of vehicular traffic throughout the year. Real-time measurements of NH₃, CO, and NO_x concentrations were conducted outside the tunnel in August (summer) and October (autumn) 2018. In August, the data were collected at 10-min intervals over a 1-month period, and the data were collected in October over every 1-h period.

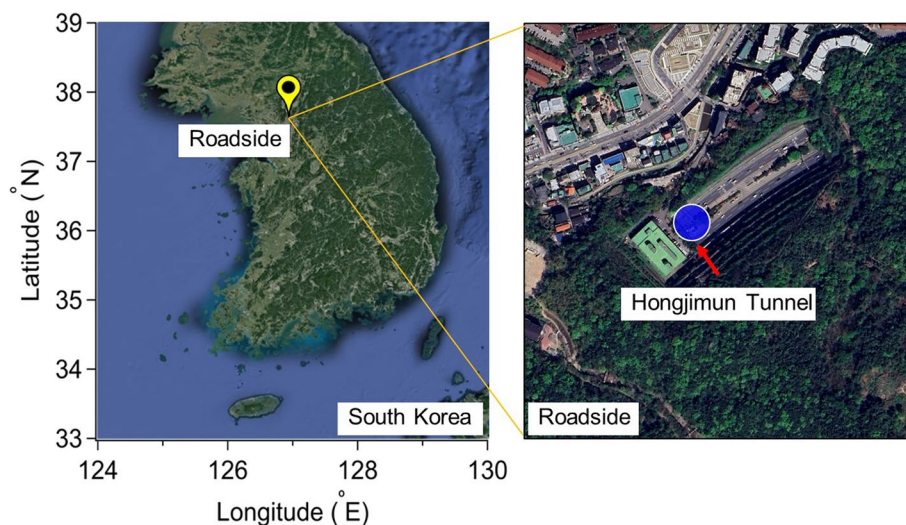


Fig. 2 Satellite images of the vehicle pollution data collection site (roadside) at Hongjimun Tunnel (37.61°N, 126.97°E), Naebu Expressway, Seoul

2.1.3 Airborne measurements over the West Sea

Two airborne measurement sorties were conducted to determine the concentration of NH_3 in the West Sea. A Beechcraft B1900D aircraft (Textron Aviation, Wichita, Kansas, USA) was flown from Taean to the West Sea of the Korean Peninsula, where a vertical spiral flight was performed to collect data on NH_3 , CO, and chemical compositions (NH_4^+ , NO_3^- , SO_4^{2-} , and organics) in non-refractory PM_{10} (NR- PM_{10}). During the spiral flight, the altitude of the aircraft varied continuously between 1200 and 300 m. While the NH_3 data were collected on June 2 and 5, 2019, the NR- PM_{10} data were collected only on June 2, 2019. The instruments recorded the data corresponding to the winds that followed different trajectories, as shown in Fig. S2a and b.

2.2 Measurement methods

2.2.1 Passive sampler

We employed the passive sampling method using Radiello NH_3 samplers (Sigma-Aldrich, St. Louis, MO, USA) for long-term measurements of NH_3 concentrations because of their appropriate features and properties (Singh et al., 2021). The sampler comprises a cylindrical tube (part number RAD1201), which acts as the diffusive body, allowing NH_3 gas particles to pass through the tube and be adsorbed by a cartridge soaked with phosphoric acid (H_3PO_3) (part number RAD168) inside the tube. The entire setup of the passive sampler was placed vertically, with the aid of a vertical adapter (part number RAD122), at a height of 2 m above the ground in an open area, and it was covered with a rain shelter (part number RAD196), as shown in Fig. S3. Temperature and humidity sensors (Lascar Electronics, UK, EasyLog USB, model

number EL-USB-2-LCD+) were attached to the setup to monitor the temperature and relative humidity during the measurement periods, as shown in Fig. S4. The NH_3 samples collected by passive sampler in the atmosphere were extracted by sonication (Hwashintech, 510 sonicate instrument) for 55 min in 10 mL of 18.2 M Ω cm deionized water, and the extracted NH_3 was analyzed using ion chromatography (Singh et al., 2021). The NH_3 concentration was calculated using a series of equations involving the physical properties of the passive sampler and the rate of NH_3 diffusion in the air (described in the Supplementary material).

2.2.2 Validation of passive samplers measurements

The accuracy of the passive samplers was cross-checked using URG denuders (URG Corporation, Chapel Hill, North Carolina, USA) installed at the Gwangju site. These URG denuders have been used widely in studies for validating passive samplers because of their ability to trap NH_3 gas from the atmosphere (Kim et al., 2021; Lee & Tsai, 2008; Li et al., 2017; Singh et al., 2021). The denuders contain a coating of phosphoric acid solution [10 g H_3PO_3 dissolved in 100 mL 18.2 M Ω cm deionized water and 900 mL methanol (CH_3OH)] to collect NH_3 gas, which is trapped on a 47 mm Teflon filter (PTFE membrane, pore size=0.45 μm , Advantec Pall Corporation, Dublin, CA, USA) pack installed in the setup. We used a vacuum pump (Thomas Piston Pump 2660 Series, Gardner Denver Thomas GmbH, Germany) to provide airflow, with the flow rate of the system regulated through an orifice (Pisco 0.4 mm Orifice, Tameson B.V., the Netherlands) and the flow rate set to 1.35 L min^{-1} . The NH_3 concentration was calculated using equations

that is provided in the [Supplementary material](#) (Eqs. S1, S2, and S3). A comparison of NH_3 concentrations measured by replicate passive samplers and between the URG denuder and passive sampler at the Gwangju site is shown in Figs. S5 and S6, respectively. The quality control of and assurance analyses for the passive sampler are provided in the [Supplementary material](#) (Fig. S7).

2.2.3 Airborne measurements over the West Sea

An aircraft modified for measuring air quality was used for collecting data on NH_3 and NR-PM_{10} concentrations over the West Sea. The Beechcraft B1900D model aircraft, owned by Hanseo University, South Korea, was flown at an altitude of 300–1200 m at a slow speed of approximately 300 km h^{-1} to collect data over the area (37.168°N , 124.200°E). The equipment components included an aerosol sampling port (Droplet Measurement Technologies, Longmont, Colorado, USA), trace gas inlets (University of California Irvine, USA), and an Aircraft Integrated Meteorological Measurement System (AIMMS-30, Aventech Research Inc., Canada) for measuring temperature, humidity, and barometric pressure. Moreover, the AIMMS-30 collects real-time location and time information using antennas installed on the aircraft (Seo et al., 2019). The NH_3 concentrations were analyzed using an EAA-30r-EP analyzer [Los Gatos Research, Inc. (LGR), San Jose, California, USA], adopting off-Axis Integrated Cavity Output Spectroscopy (OA-ICOS) technology. The chemical compositions (NH_4^+ , NO_3^- , SO_4^{2-} , and organics) in NR-PM_{10} were measured using a high-resolution time-of-flight aerosol mass spectrometer (HR-TOF-AMS, Aerodyne Research Inc, Billerica, Massachusetts, USA). In addition, a Serinus 30 CO analyzer (Acoem Ecotech, Australia) was used for measuring the vertical profile in the CO concentration over the West Sea. Back trajectory analysis of the air recorded in the area was conducted for accurate estimation of the path of the wind transporting the pollutants. The Hybrid Single-Particle Lagrangian Integrated Trajectory model of the Air Resources Laboratory (ARL, US National Oceanic and Atmospheric Administration) was used for back trajectory analysis at 2-h intervals over a 72-h period on each of the two data recording dates (Draxler & Hess, 1997; Rolph et al., 2017; Stein et al., 2015).

3 Results and discussion

3.1 Concentrations of NH_3 at six supersites

As shown in Fig. 3, the mean NH_3 concentration measured at the Seoul site was 5.6 ± 2.4 ppb, whereas that of the Daejeon region was higher at 9.0 ± 3.4 ppb. The Gwangju region recorded the highest NH_3 concentration (9.3 ± 3.3 ppb). The mean NH_3 concentrations in the Ulsan region, Jeju Island, and Baengnyeong Island were

3.5 ± 1.4 , 2.1 ± 1.8 , and 1.3 ± 1.1 ppb, respectively. The regional variations of NH_3 concentration, temperature, and relative humidity measured from 2020 to 2021 are shown in Figs. S8 and S9. Interestingly, despite the large and dense population of Seoul, the NH_3 concentrations at the Seoul site were lower than those in the Gwangju and Daejeon regions, probably ascribable to the agricultural and industrial activities near these sites. Gwangju, located close to a sanitary treatment plant and agricultural land, showed the highest NH_3 concentrations of all the study sites. The Daejeon site, surrounded primarily by agricultural areas, also showed a high concentration of NH_3 . The lower NH_3 concentrations at Baengnyeong and Jeju islands were attributed to their lower population numbers and minimal industrial activities. The NH_3 concentrations in other regions, such as Seoul and Ulsan, showed a direct proportional relationship to their respective populations, indicating the contributions of diverse human, industrial, traffic, and agricultural activities to NH_3 emissions. These findings highlighted the need for targeted control measures in areas with high NH_3 concentrations to mitigate their effects on human health and air quality.

3.2 Seasonal variation in NH_3 concentrations

We used the following definitions for the four seasons, namely spring (March 1 to May 31), summer (June 1 to August 31), autumn (September 1 to November 30), and winter (December 1 to February 28). The study results presented in Fig. 4 show distinct seasonal patterns across all the sites. The Seoul and Daejeon sites showed the highest NH_3 concentration during summer (Seoul 7.5 ± 2.3 ppb, Daejeon 11.6 ± 3.3 ppb) and the lowest during winter (Seoul 3.2 ± 1.3 ppb, Daejeon 5.6 ± 2.6 ppb). The Gwangju and Ulsan sites and Baengnyeong Island also showed the highest NH_3 concentration during summer (Gwangju 11.1 ± 4.4 ppb, Ulsan 4.1 ± 1.3 ppb, Baengnyeong Island 2.1 ± 1.6 ppb). However, the highest NH_3 concentration at Jeju Island was recorded during spring (3.1 ± 1.6 ppb).

Various factors could cause the observed seasonality in NH_3 concentrations, including temperature, rainfall, and agricultural activities. During the summer months, high temperatures and increased agricultural activity in mainland South Korea leads to the decomposition of organic fertilizers, which caused the highest NH_3 concentrations across most of our study sites except Jeju Island (Kuttipurath et al., 2020). Moreover, high temperatures caused the conversion of aqueous NH_3 to the gaseous phase. In contrast, wet deposition during rainfall in the autumn and winter seasons was responsible for the lowest NH_3 concentrations during winter at most study sites (Warner

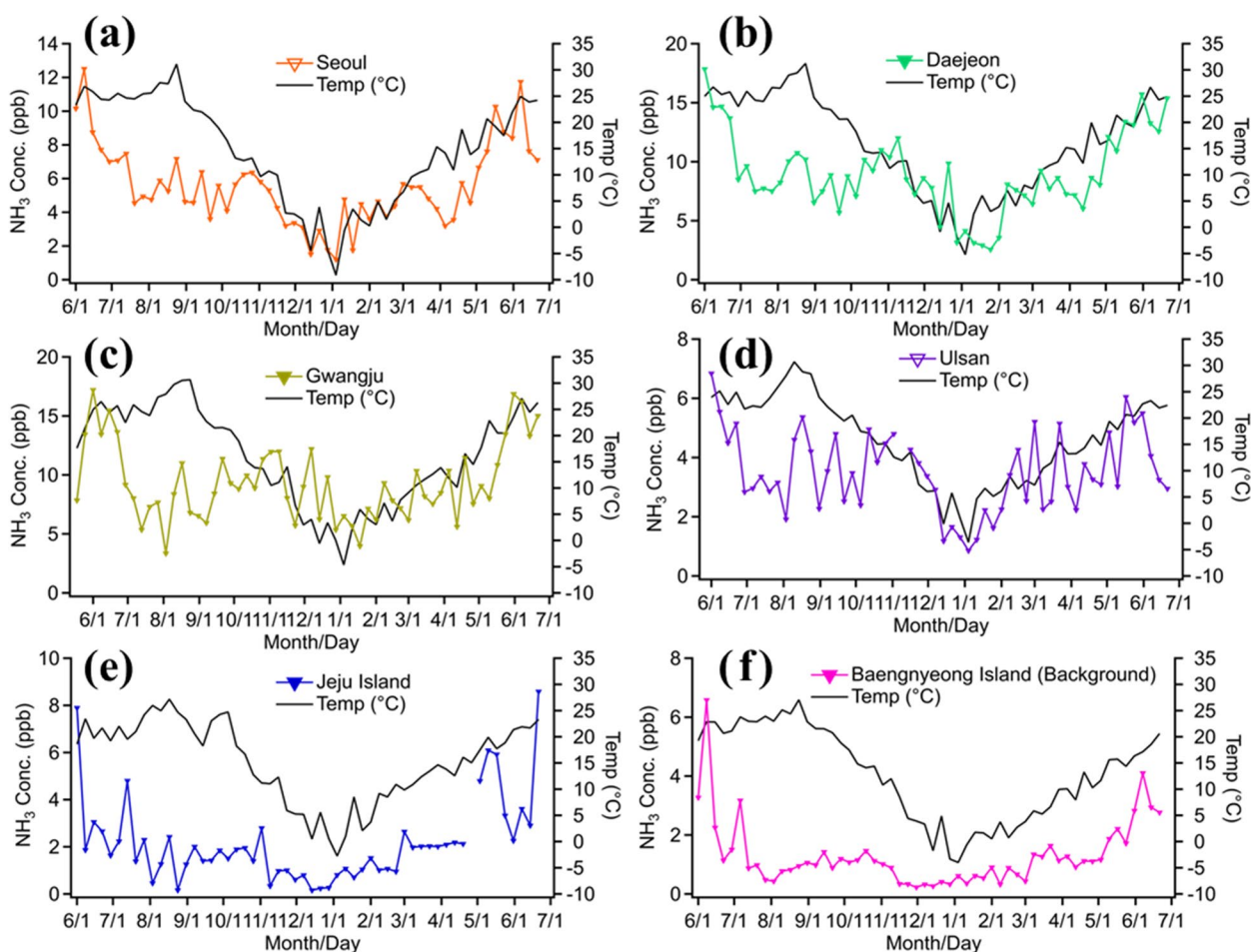


Fig. 3 Spatial distributions of weekly NH_3 concentrations and temperatures at various National Institute of Environmental Research (NIER) supersites over 1 year (2020–2021). **a** Seoul, **b** Daejeon, **c** Gwangju, **d** Ulsan, **e** Jeju Island, **f** Baengnyeong Island (background)

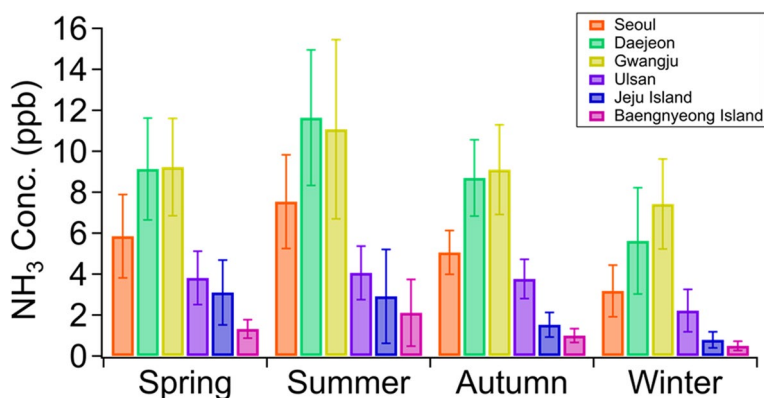


Fig. 4 Seasonal variation in NH_3 concentrations at various National Institute of Environmental Research (NIER) supersites over 1 year (2020–21)

et al., 2016). Further, NH_3 reacts with HNO_3 in the atmosphere during the colder months, leading to a further reduction in atmospheric NH_3 concentrations (Zhou et al., 2019).

Jeju Island was the exception to the observed seasonal trend, with the highest NH_3 concentration recorded during the spring season. This phenomenon could be ascribed to the agricultural activities during the spring

season contributing to the higher NH₃ concentrations. In addition, the relatively lower summer temperatures on the island compared with other regions around South Korea could have contributed to the higher NH₃ concentrations recorded in spring. The results of this study showed the importance of understanding the seasonal variability in and factors contributing to NH₃ concentrations. This information could inform targeted control measures to mitigate the effects of NH₃ emissions on human health and air quality.

3.3 Seasonal variation in roadside emissions

Several sources influence the concentration of NH₃ in the atmosphere, with vehicle emissions being a significant contributor. In this section, the seasonal variation in the correlation between NH₃, CO, and NO_x concentrations from vehicle emissions at roadsides in Seoul is discussed. The study was conducted over a 1-month period each during two seasons, namely summer (August) and autumn (October) in 2018. The NH₃, CO, and NO_x concentrations were measured and the data analyzed using correlation coefficient (R^2) values. The results showed that during summer, a strong positive correlation ($R^2=0.62$) existed between the CO and NH₃ concentrations, indicating that the NH₃ emissions were consistent with the CO emissions from vehicles (Fig. 5a). A strong correlation ($R^2=0.69$) was also observed between the NO_x and NH₃ concentrations during the same season. These results suggested that NH₃ emissions from vehicles were a significant contributor to air pollution in Seoul during summer.

During autumn, a positive correlation ($R^2=0.61$) was observed between the CO and NH₃ concentrations similar to summer, and weaker positive correlation ($R^2=0.62$) was observed between NO_x and NH₃ concentrations

than in summer. The concentrations of NH₃, CO, and NO_x emissions were consistent with each other, as shown in Fig. 5b, and most NH₃ pollution recorded at the site during autumn could be ascribed to vehicle emissions. These findings suggested that vehicle emissions during summer and autumn (particularly summer) contributed substantially to NH₃ pollution at Seoul roadsides. Therefore, appropriate measures are required to reduce vehicle emissions and improve the air quality of the city.

3.4 Seasonal variation in the correlation between NH₃ and NO₂ at the Seoul supersite

As noted in Section 3.3, NH₃ emissions along roadsides in Seoul were affected significantly by vehicle emissions; however, NO₂ is another major air pollutant deriving from such emissions. To improve our understanding of the correlation between NH₃ and NO₂, we investigated the concentrations at the supersite in Seoul over a 1-month period during three seasons, namely winter (January), spring (March), and summer (August) in 2020–2021. Figure 6 shows the correlation between NO₂ and NH₃. In winter, a correlation coefficient value of $R^2=0.584$ was observed between NO₂ and NH₃ concentrations, i.e., the concentrations of NH₃ and NO₂ were consistent, suggesting that vehicle emissions were the major source of NH₃ pollution during that season (Fig. 6c). However, in spring and summer, the correlation coefficient between NO₂ and NH₃ were 0.007 and 0.004, respectively (Fig. 6a and b). It suggests a considerable increase in the NH₃ concentration without NO₂ increase. This increase in the NH₃ concentration without NO₂ may be due to increased agricultural activity from spring to summer in the nearby regions or other influences than the effect of vehicle emissions. Overall, our study

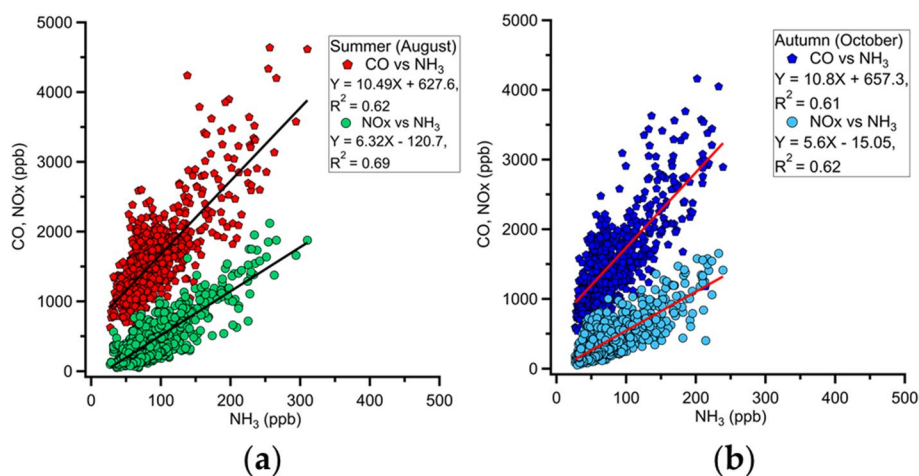


Fig. 5 Correlations between CO and NO_x with NH₃ at roadside in Seoul during **a** summer and **b** autumn

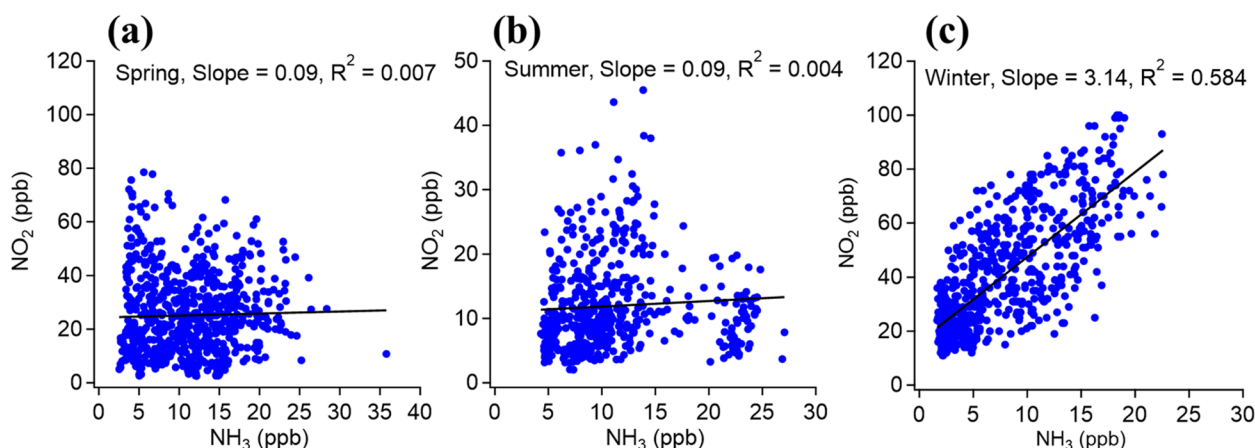


Fig. 6 Correlations between NO_2 and NH_3 at the supersite in Seoul during **a** spring, **b** summer, and **c** winter

confirmed that NH_3 emissions in Seoul were affected significantly by vehicle emissions, with agricultural activities playing an important role in increasing NH_3 concentrations during the summer season.

3.5 Vertical distribution of NH_3 and NR- PM_{10} over the West Sea

Airborne measurements were conducted over the West Sea of South Korea to determine the sources of gaseous emissions, particularly long-range transported and maritime emissions. The long-range transportation measurements were conducted on 2 June 2019, with the results shown in Fig. 7a and b. The spiral flight provided vertical profiles of various NR- PM_{10} chemical compositions based on their concentrations. The concentrations of NO_3^- were the lowest ($0.26\text{--}1.10\ \mu\text{g m}^{-3}$) at altitudes of 300–1000 m, with the concentrations of NH_4^+ being slightly higher ($0.90\text{--}1.32\ \mu\text{g m}^{-3}$) than those of NO_3^- at these altitudes. Higher organics concentrations were observed ($1.7\text{--}3.2\ \mu\text{g m}^{-3}$) compared with those of NH_4^+ at altitudes of 300–1000 m, whereas the SO_4^{2-} concentrations were higher ($3.22\text{--}3.89\ \mu\text{g m}^{-3}$) than the organics concentrations at this altitude range. The CO concentrations range was 198.1–295.59 ppbv at altitude range 300–1000 m, with NR- PM_{10} showing a similar trend. We employed CO as a tracer for tracking long-range pollutant transport. As the altitude increased beyond 1000 m, the concentrations of NO_3^- exceeded those of NH_4^+ , whereas the other components retained their order. The NH_3 concentration range was 7.91–14.2 ppbv, increasing along with the altitude range of 300–1000 m, with the recorded concentrations at the highest altitude of 1103.5 m being $12.24\ \mu\text{g m}^{-3}$ (SO_4^{2-}), $10.86\ \mu\text{g m}^{-3}$ (organics), $8.21\ \mu\text{g m}^{-3}$ (NO_3^-), $5.91\ \mu\text{g m}^{-3}$ (NH_4^+), 310.8 ppbv (CO), and 15.7 ppbv (NH_3). These results

indicated that the pollutant concentrations increased along with the altitude increasing above sea level, implying that the primary source of pollution over the West Sea on 2 June 2019 was long-range transportation from neighboring regions such as northeastern China. Back trajectory analysis of the wind confirmed that it was blowing from China toward the West Sea. The correlation between altitude and temperature indicated that the temperature dropped below $20\ ^\circ\text{C}$ as the height increased over 400 m. These results suggested no possibility of NH_3 emissions deriving from the decomposition of NH_4NO_3 (Chaturvedi & Dave, 2013).

The maritime NH_3 emissions were measured over the West Sea on 5 June 2019, with the results shown in Fig. 7b. The NH_3 concentration decreased from 10.1 to 7.37 ppbv as the height increased from 300 to 1000 m, indicating that most NH_3 derived from oceanic emissions near the ocean surface (Paulot et al., 2015). Figure S10 shows that the temperature increased over $20\ ^\circ\text{C}$ as the altitude increased over 400 m, implying that NH_4NO_3 decomposition could have contributed additional NH_3 to the oceanic emissions.

4 Conclusions

The aim of this study was analyzing the trends of NH_3 emissions in the South Korean Peninsula and West Sea region and identifying the factors causing the pollution. The data on NH_3 and other air pollutants (NO_x , CO, and NR- PM_{10}) were collected from six supersites across the peninsula, a roadside in Seoul, and the West Sea over different periods, ranging from 1 month to 1 year.

In synthesizing the results obtained from each site, the complex interplay of agricultural, urban, and oceanic factors influences the NH_3 emissions in the South Korean Peninsula and West Sea region.

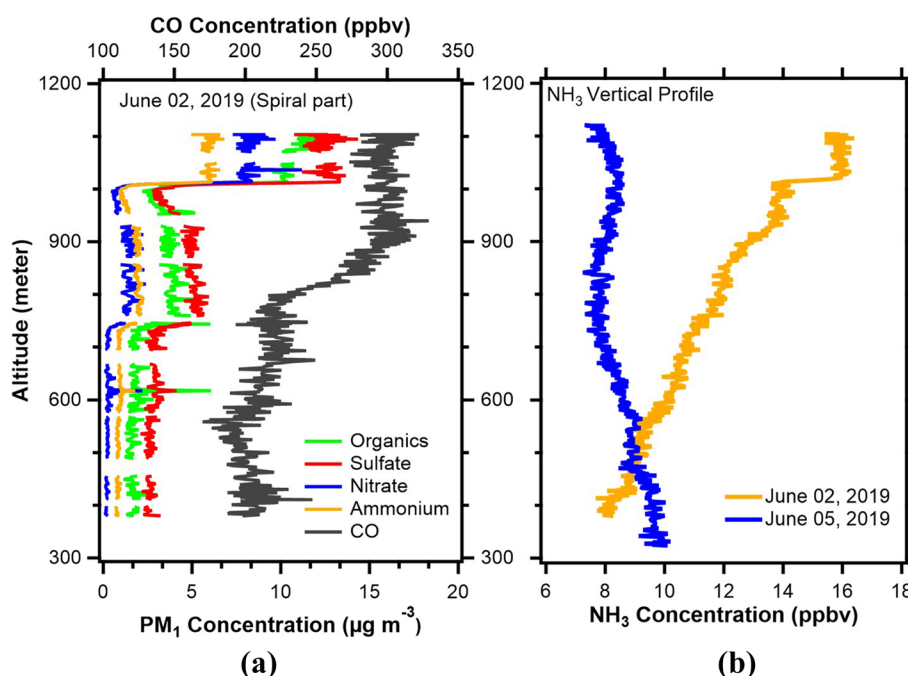


Fig. 7 Vertical profiles of **a** CO and particulate matter [aerodynamic diameter $\leq 1 \mu\text{m}$ (PM_{10})] concentrations by their compositions recorded on 2 June 2019 during long-range transport; **b** NH_3 concentrations measured over the West Sea on 2 June (long-range transport) and 5 June 2019 (ocean origin)

In rural areas, the high concentrations of NH_3 were primarily attributed to agricultural activities, especially using fertilizers. This resulted in the decomposition of NH_4NO_3 during the high summer temperatures, highlighting the direct impact of agricultural practices on ambient NH_3 concentration. Conversely, areas with lower populations showed the lowest NH_3 concentrations due to the absence of significant agricultural, industrial, or anthropogenic activities.

In contrast, at urban sites like Seoul, there was a clear correlation between ambient NH_3 and vehicle emissions, which suggests that vehicle emission is important to NH_3 pollution in urban. Interestingly, this correlation was particularly strong during winter, implying that urban vehicle emissions were a primary source of NH_3 during this season. But, increasing the NH_3 concentrations observed during spring and summer suggest that additional NH_3 sources, beyond vehicle emissions, are likely tied to agricultural activities within or near the city.

Lastly, the airborne measurement over the West Sea of South Korea revealed that a significant portion of NH_3 pollution originated from oceanic emissions and NH_4NO_3 decomposition by high temperature, and long-range transportation from the northeastern region of China.

This interconnectedness of rural, urban, and maritime influences explains the complexities of understanding

and managing NH_3 emissions. It underscores the need for comprehensive, multi-faceted strategies considering the varied emission sources and environmental dynamics in different regions and seasons. In conclusion, the results of our study provided valuable insights into the emission sources of NH_3 in primary air pollutants in South Korea, highlighting the contributions of both land-based and oceanic sources. These findings could help inform policymakers and stakeholders for developing effective air pollution control strategies in the region.

Supplementary Information

The online version contains supplementary material available at <https://doi.org/10.1007/s44273-023-00008-7>.

Additional file 1: Fig. S1. Experimental setup for vehicular emission data collection at the roadside site Naebu Expressway near Hongjimun Tunnel (37.61°N, 126.97°E), Seoul Metropolitan Area. **Fig. S2.** Backward trajectory analysis for (a) long-range transportation (June 2, 2019) and (b) maritime origin of West Sea. **Fig. S3.** Ambient NH_3 was collected using Radiello passive samplers installed at all the sites. **Fig. S4.** Real-time installation of the NH_3 passive sampler with temperature (°C) and relative humidity (%) sensor at six supersites. **Fig. S5.** Comparison of NH_3 concentrations measured by replicates passive samples. Error bars represent the relative standard deviation of 3.3 % calculated from all 168 pooled replicate samples. **Fig. S6.** Comparison of NH_3 concentrations between the Radiello passive samplers and denuder samplers at the Gwangju (Honam region) ($N = 27$). **Fig. S7.** Sample analysis for accuracy, precision, and minimum detection limit (MDL). **Fig. S8.** Time-series of NH_3 concentration for all six supersites in the South Korea from June 1st, 2020, to July 1st, 2021. All samples were measured every Monday for sampling on a weekly basis. **Fig. S9.** Regional

distribution of temperature (°C) and relative humidity (%) information over the period of 1 year on a weekly average basis. **Fig. S10.** Vertical profiles of temperature on June 2 and June 5, 2019, over the West Sea. **Table S1.** Quality assurance and quality control (QA/QC) of ion chromatography during NH₃ sample analysis.

Acknowledgements

This work was supported by a grant from the National Institute of Environment Research (NIER), funded by the Ministry of Environment (MOE) of the Republic of Korea (grant no. NIER-2019-04-02-018). The extended experiment was supported by a grant from the Korea Basic Science Institute (National Research Facilities and Equipment Center), funded by the Ministry of Education (grant no. 2019R1A6C1020041). Additional data processing was supported by the National Research Foundation of Korea (grant no. 2020M3G1A1114997) and the Ministry of Science and ICT (grant no. 2019M1A2A2103953).

Authors' contributions

Writing – Original Draft: Taehyun Park, Rahul Singh, Taehyoung Lee and Jinsoo Choi; Writing - review and editing: Min-Suk Bae, Hae-Jin Jung and Jongtae Lee; Formal analysis: Jihee Ban, Kyunghoon Kim and Taehyun Park; Methodology: Gyutae Park and Dong-Gil Yu; Visualization: Siyoung Choi and Jeongin Song; Validation: Seokwon Kang and Rahul Singh; Conceptualization: Taehyoung Lee and Jinsoo Choi; Supervision: Jinsoo Choi, Junyoung Ahn and Taehyoung Lee; Investigation: Yunsung Lim and Dong-Gil Yu; Project administration: Yong-Jae Lim, Hye Jung Shin and Jinsoo Park; Resources: Hyun Woong Kim, Tae Kyung Hwang, Yu Jin Choi, Soo-Young Kim, Hyo Seon Kim and Yu woon Chang.

Availability of data and materials

The datasets generated during and/or analyzed during the current study are available from the corresponding author on reasonable request.

Declarations

Competing interests

The authors declare that they have no known competing financial interests or personal relationships that could have appeared to influence the work reported in this paper.

Received: 14 April 2023 Accepted: 23 June 2023

Published online: 18 July 2023

References

- Badr, O., & Probert, S. D. (1994). Sources of atmospheric carbon monoxide. *Applied Energy*, *49*, 145–195. [https://doi.org/10.1016/0306-2619\(94\)90036-1](https://doi.org/10.1016/0306-2619(94)90036-1)
- Cao, H., Henze, D. K., Cady-Pereira, K., McDonald, B. C., Harkins, C., Sun, K., Bowman, K. W., Fu, T.-M., & Nawaz, M. O. (2021). COVID-19 lockdowns afford the first satellite-based confirmation that vehicles are an under-recognized source of urban NH₃ pollution in Los Angeles. *Environmental Science & Technology Letters*, *9*, 3–9. <https://doi.org/10.1021/acs.estlett.1c00730>
- Chang, Y., Zou, Z., Deng, C., Huang, K., Collett, J. L., Lin, J., & Zhuang, G. (2016). The importance of vehicle emissions as a source of atmospheric ammonia in the megacity of Shanghai. *Atmospheric Chemistry and Physics*, *16*, 3577–3594. <https://doi.org/10.5194/acp-16-3577-2016>
- Chaturvedi, S., & Dave, P. N. (2013). Review on thermal decomposition of ammonium nitrate. *Journal of Energetic Materials*, *31*, 1–26. <https://doi.org/10.1080/07370652.2011.573523>
- Clark, L. P., Sreekanth, V., Bekbulat, B., Baum, M., Yang, S., Baylon, P., Gould, T. R., Larson, T. V., Seto, E. Y. W., Space, C. D., & Marshall, J. D. (2020). Developing a low-cost passive method for long-term average levels of light-absorbing carbon air pollution in polluted indoor environments. *Sensors*, *20*, 3417. <https://doi.org/10.3390/s20123417>
- Draxler, R. R., & Hess, G. (1997). *Description of the HYSPPLIT4 modeling system*.
- Huang, X., Qiu, R., Chan, C. K., & Ravi Kant, P. (2011). Evidence of high PM_{2.5} strong acidity in ammonia-rich atmosphere of Guangzhou, China: Transition in pathways of ambient ammonia to form aerosol ammonium at [NH₄⁺]/[SO₄²⁻]=1.5. *Atmospheric Research*, *99*, 488–495. <https://doi.org/10.1016/j.atmosres.2010.11.021>
- Kang, S., Park, G., Park, T., Ban, J., Kim, K., Seo, Y., Choi, J., Seo, S., Choi, J., Bae, M.-S., & Lee, T. (2020). Semi-continuous measurements of water-soluble organic carbon and ionic composition of PM 2.5 in Baengnyeong Island during the 2016 KORUS-AQ (Korea-United States Air Quality Study). *Asian Journal of Atmospheric Environment*, *14*, 307–318. <https://doi.org/10.5572/ajae.2020.14.3.307>
- Kim, K., Park, G., Kang, S., Singh, R., Song, J., Choi, S., Park, I., Yu, D.-G., Kim, M.-B., Bae, M.-S., Jung, S., Chang, Y., Park, J., Jung, H.-J., Lim, Y.-J., & Lee, T. (2021). The comparisons of real-time ammonia adsorption measurement in varying inlet tubes and the different ammonia measurement methods in the atmosphere. *Asian Journal of Atmospheric Environment*, *15*, 93–102. <https://doi.org/10.5572/ajae.2021.139>
- Kumar, A., Patil, R. S., Dikshit, A. K., & Kumar, R. (2019). Assessment of spatial ambient concentration of NH₃ and its health impact for Mumbai city. *Asian Journal of Atmospheric Environment*, *13*, 11–19. <https://doi.org/10.5572/ajae.2019.13.1.011>
- Kuttippurath, J., Singh, A., Dash, S. P., Mallick, N., Clerbaux, C., Van Damme, M., Clarisse, L., Coheur, P. F., Raj, S., Abhishek, K., & Varikoden, H. (2020). Record high levels of atmospheric ammonia over India: Spatial and temporal analyses. *Science of The Total Environment*, *740*, 139986. <https://doi.org/10.1016/j.scitotenv.2020.139986>
- Lee, I. S., & Tsai, S.-W. (2008). Passive sampling of ambient ozone by solid phase microextraction with on-fiber derivatization. *Analytica Chimica Acta*, *610*, 149–155. <https://doi.org/10.1016/j.jaca.2008.01.035>
- Lee, T., Choi, J., Lee, G., Ahn, J., Park, J. S., Atwood, S. A., Schurman, M., Choi, Y., Chung, Y., & Collett, J. L. (2015). Characterization of aerosol composition, concentrations, and sources at Baengnyeong Island, Korea using an aerosol mass spectrometer. *Atmospheric Environment*, *120*, 297–306. <https://doi.org/10.1016/j.atmosenv.2015.08.038>
- Li, Y., Thompson, T. M., Van Damme, M., Chen, X., Benedict, K. B., Shao, Y., Day, D., Boris, A., Sullivan, A. P., Ham, J., Whitburn, S., Clarisse, L., Coheur, P. F., & Collett, J. L., Jr. (2017). Temporal and spatial variability of ammonia in urban and agricultural regions of northern Colorado, United States. *Atmospheric Chemistry and Physics*, *17*, 6197–6213. <https://doi.org/10.5194/acp-17-6197-2017>
- Liu, T., Wang, X., Wang, B., Ding, X., Deng, W., Lü, S., & Zhang, Y. (2014). Emission factor of ammonia (NH₃) from on-road vehicles in China: Tunnel tests in urban Guangzhou. *Environmental Research Letters*, *9*, 064027. <https://doi.org/10.1088/1748-9326/9/6/064027>
- Miller, D. C., Poucher, S., Cardin, J. A., & Hansen, D. (1990). The acute and chronic toxicity of ammonia to marine fish and a mysid. *Archives of Environmental Contamination and Toxicology*, *19*, 40–48. <https://doi.org/10.1007/BF01059811>
- Mukhopadhyay, K., & Forssell, O. (2005). An empirical investigation of air pollution from fossil fuel combustion and its impact on health in India during 1973–1974 to 1996–1997. *Ecological Economics*, *55*, 235–250. <https://doi.org/10.1016/j.ecolecon.2004.09.022>
- Park, J., Kim, E., Oh, S., Kim, H., Kim, S., Kim, Y. P., & Song, M. (2021). Contributions of ammonia to high concentrations of PM_{2.5} in an urban area. *Atmosphere*, *12*, 1676. <https://doi.org/10.3390/atmos12121676>
- Paulot, F., Jacob, D. J., Johnson, M. T., Bell, T. G., Baker, A. R., Keene, W. C., Lima, I. D., Doney, S. C., & Stock, C. A. (2015). Global oceanic emission of ammonia: Constraints from seawater and atmospheric observations. *Global Biogeochemical Cycles*, *29*, 1165–1178. <https://doi.org/10.1002/2015GB005106>
- Perrone, M. R., Dinioi, A., Becagli, S., & Udisti, R. (2014). Chemical composition of PM₁ and PM_{2.5} at a suburban site in southern Italy. *International Journal of Environmental Analytical Chemistry*, *94*, 127–150. <https://doi.org/10.1080/03067319.2013.791978>
- Puchalski, M. A., Sather, M. E., Walker, J. T., Lehmann, C. M. B., Gay, D. A., Mathew, J., & Robarge, W. P. (2011). Passive ammonia monitoring in the United States: Comparing three different sampling devices. *Journal of Environmental Monitoring*, *13*, 3156–3167. <https://doi.org/10.1039/C1EM10553A>
- Rolph, G., Stein, A., & Stunder, B. (2017). Real-time Environmental Applications and Display sYstem: READY. *Environmental Modelling & Software*, *95*, 210–228. <https://doi.org/10.1016/j.envsoft.2017.06.025>

- Seo, B.-K., Park, S. B., Lee, D., Yu, M., Yu, J., Bae, K.-N., Ahn, J., Park, J., Kim, S., Lee, T., & Kim, J. (2019). Airborne inlets and instrumentation on aircraft platform for air quality observation. *Journal of Korean Society for Atmospheric Environment*, 35, 815–830. <https://doi.org/10.5572/KOSAE.2019.35.6.815>
- Seoul Research Data Service. Population growth. Available at: <https://data.si.re.kr/data/%ED%86%B5%EA%B3%84%EB%A1%9C-%EB%B3%B8-%EC%84%9C%EC%9A%B8-%EC%98%81%EB%AC%B8%ED%8C%90/325>. Accessed 20 Feb 2023.
- Sigurdarson, J. J., Svane, S., & Karring, H. (2018). The molecular processes of urea hydrolysis in relation to ammonia emissions from agriculture. *Reviews in Environmental Science and Bio/technology*, 17, 241–258. <https://doi.org/10.1007/s11157-018-9466-1>
- Singh, R., Kim, K., Park, G., Kang, S., Park, T., Ban, J., Choi, S., Song, J., Yu, D.-G., Woo, J.-H., Choi, Y., & Lee, T. (2021). Seasonal and spatial variations of atmospheric ammonia in the urban and suburban environments of Seoul, Korea. *Atmosphere*, 12, 1607. <https://doi.org/10.3390/atmos12121607>
- Stein, A. F., Draxler, R. R., Rolph, G. D., Stunder, B. J. B., Cohen, M. D., & Ngan, F. (2015). NOAA's HYSPLIT atmospheric transport and dispersion modeling system. *Bulletin of the American Meteorological Society*, 96, 2059–2077. <https://doi.org/10.1175/bams-d-14-00110.1>
- Stern, A. C. (2015). *Air pollution VI: Air pollutants, their transformation and transport*. Elsevier.
- Tsai, W. Y., Chan, L. Y., Blake, D. R., & Chu, K. W. (2006). Vehicular fuel composition and atmospheric emissions in South China: Hong Kong, Macau, Guangzhou, and Zhuhai. *Atmospheric Chemistry and Physics*, 6, 3281–3288. <https://doi.org/10.5194/acp-6-3281-2006>
- Wang, S., Nan, J., Shi, C., Fu, Q., Gao, S., Wang, D., Cui, H., Saiz-Lopez, A., & Zhou, B. (2015). Atmospheric ammonia and its impacts on regional air quality over the megacity of Shanghai, China. *Scientific Reports*, 5, 15842. <https://doi.org/10.1038/srep15842>
- Wang, M., Kong, W., Marten, R., He, X.-C., Chen, D., Pfeifer, J., Heitto, A., Kontkanen, J., Dada, L., Kürten, A., Yli-Juuti, T., Manninen, H. E., Amanatidis, S., Amorim, A., Baalbaki, R., Baccarini, A., Bell, D. M., Bertozzi, B., Bräkling, S., ... Donahue, N. M. (2020). Rapid growth of new atmospheric particles by nitric acid and ammonia condensation. *Nature*, 581, 184–189. <https://doi.org/10.1038/s41586-020-2270-4>
- Warner, J. X., Wei, Z., Strow, L. L., Dickerson, R. R., & Nowak, J. B. (2016). The global tropospheric ammonia distribution as seen in the 13-year AIRS measurement record. *Atmospheric Chemistry and Physics*, 16, 5467–5479. <https://doi.org/10.5194/acp-16-5467-2016>
- Zhang, Y., Ding, Z., Xiang, Q., Wang, W., Huang, L., & Mao, F. (2020). Short-term effects of ambient PM1 and PM2.5 air pollution on hospital admission for respiratory diseases: Case-crossover evidence from Shenzhen, China. *International Journal of Hygiene and Environmental Health*, 224, 113418. <https://doi.org/10.1016/j.ijheh.2019.11.001>
- Zhao, D., Chen, H., Shao, H., & Sun, X. (2018). Vehicle emission factors for particulate and gaseous pollutants in an urban tunnel in Xi'an, China. *Journal of Chemistry*, 2018, 8964852. <https://doi.org/10.1155/2018/8964852>
- Zhou, C., Zhou, H., Holsen, T. M., Hopke, P. K., Edgerton, E. S., & Schwab, J. J. (2019). Ambient ammonia concentrations across New York State. *Journal of Geophysical Research: Atmospheres*, 124, 8287–8302. <https://doi.org/10.1029/2019JD030380>

Publisher's Note

Springer Nature remains neutral with regard to jurisdictional claims in published maps and institutional affiliations.